Titanium Diboride Thin Films by Low-Temperature Chemical Vapor Deposition from the Single Source Precursor $Ti(BH_4)_3$(1,2-dimethoxyethane)

Navneet Kumar,[†,‡] Yu Yang,[†,‡] Wontae Noh,[§,‡] Gregory S. Girolami,*[,‡,§] and John R. Abelson*[,†,‡]

Department of Materials Science and Engineering, University of Illinois at Urbana Champaign, 1304 West Green Street, Urbana, Illinois 61801, Department of Chemistry, University of Illinois at Urbana Champaign, 600 South Mathews Avenue, Urbana, Illinois 61801, and Frederick Seitz Materials Research Laboratory, 104 South Goodwin Avenue, Urbana, Illinois 61801

Received January 29, 2007. Revised Manuscript Received May 7, 2007

Titanium diboride is a technologically important refractory conductor with a melting point of 3220 °C, a high electrical conductivity, and good wear and corrosion resistance. Thin films of TiB_2 have been obtained at temperatures as low as 170 °C by thermal chemical vapor deposition from the halogen-free single-source precursor $Ti(BH_4)_3(CH_3OCH_2CH_2OCH_3)$. Films deposited at temperatures below 200 °C are near stoichiometric, free of impurities, and amorphous as judged by X-ray diffraction. These films exhibit dense nucleation, including on SiO_2 substrates, and have root-mean-square roughness, as measured by atomic force microscopy, of less than 1 nm for films 5−60 nm thick. At growth temperatures between 200 and 600 °C, the films are still amorphous but contain 12−15 atomic % oxygen and 15−20 atomic % carbon; these impurities are incorporated at the expense of boron. For growth at 800 °C and above, the films are crystalline, stoichiometric, and free of impurities. These high-temperature films are oriented in a preferred fashion with respect to the substrate: on Si(100) the films have a (101) orientation when grown at 800 °C but a (001) orientation when the films are grown at 900 °C. An amorphous TiB_2 film, grown at 175 °C to a thickness of 7 nm, performs well as a diffusion barrier: no Cu diffuses across the TiB_2 after thermal annealing at 600 °C for 30 min.

Introduction

Titanium diboride is a high performance metallic ceramic whose properties surpass those of transition metal nitride and carbide counterparts:[1] it has a high melting point (3220 °C), a high mechanical hardness, excellent wear properties, and excellent corrosion resistance toward molten metals. In addition, it has a low electrical resistivity of 6 $\mu\Omega\cdot$cm for single crystal and 10 $\mu\Omega\cdot$cm for polycrystalline forms.[2] TiB_2 is an attractive material for use as a hard coating for cutting tools,[3] as an electrode[4] and a diffusion barrier material[5,6] in microelectronics, and as a substrate to grow superconducting MgB_2 thin films.[7] Thin films of TiB_2 have been deposited both by sputtering[8−10] and chemical vapor deposition (CVD) routes.[2,11−13] An inherent shortcoming of sputtering is its nonconformal nature. Previous CVD routes, all of which involve halide based precursors, have several disadvantages including high growth temperatures of 600 °C or greater and the production of corrosive byproducts. In this paper we report a detailed study of a halide free and low-temperature CVD route to deposit smooth, conducting, and conformal TiB_2 films from the single source precursor tris(tetrahydroborato)-(1,2-dimethoxyethane)titanium(III), hereafter termed Ti-$(BH_4)_3$(dme). The synthesis of this compound and a preliminary investigation of its use as a CVD precursor was reported previously by one of us.[14]

Experiment

1. Precursor Preparation. The $Ti(BH_4)_3$(dme) precursor is prepared by treating titanium tetrachloride with excess sodium

* To whom correspondence should be addressed. E-mail: girolami@scs.uiuc.edu (G.S.G.), abelson@mrl.uiuc.edu (J.R.A.).

† Department of Materials Science and Engineering, University of Illinois at Urbana Champaign.

‡ Frederick Seitz Materials Research Laboratory.

§ Department of Chemistry, University of Illinois at Urbana Champaign.

(1) Holleck, H. *J. Vac. Sci. Technol. A* **1986**, *4*, 2661−2669.
(2) Choi, C. S.; Xing, G. C.; Ruggles, G. A.; Osburn, C. M. *J. Appl. Phys.* **1991**, *69*, 7853−7861.
(3) Mitterer, C. *J. Solid State Chem.* **1997**, *133*, 279−291.
(4) Ranjit, R.; Zagozdzon-Wosik, W.; Rusakova, I.; van der Heide, P.; Zhang, Z. H.; Bennett, J.; Marton, D. *Rev. Adv. Mater. Sci.* **2004**, *8*, 176−184.
(5) Shappirio, J.; Finnegan, J.; Lux, R.; Fox, D.; Kwiatkowski, J.; Kattelus, H.; Nicolet, M. *J. Vac. Sci. Technol. A* **1985**, *3*, 2255−2258.
(6) Chen, J. S.; Wang, J. L. *J. Electrochem. Soc.* **2000**, *147*, 1940−1944.
(7) Zhai, H. Y.; Christen, H. M.; Cantoni, C.; Goyal, A.; Lowndes, D. H. *Appl. Phys. Lett.* **2002**, *80*, 1963−1965.
(8) Berger, M.; Larsson, M.; Hogmark, S. *Surf. Coat. Technol.* **2000**, *124*, 253−261.
(9) Shutou, A.; Matsui, T.; Tsuda, H.; Mabuchi, H.; Morii, K. *Mater. Lett.* **2000**, *45*, 143−148.
(10) Ye, J.; Ulrich, S.; Sell, K.; Leiste, H.; Stuber, M.; Holleck, H. *Surf. Coat. Technol.* **2003**, *174*, 959−963.
(11) Vandervalk, H. J. L.; Grondel, J. H. F. *Solid State Ionics* **1985**, *16*, 99−104.
(12) Motojima, S.; Hotta, H. *J. Less-Common Met.* **1988**, *141*, 327−333.
(13) Pierson, H. O.; Mullendore, A. W. *Thin Solid Films* **1982**, *95*, 99−104.
(14) Jensen, J. A.; Gozum, J. E.; Pollina, D. M.; Girolami, G. S. *J. Am. Chem. Soc.* **1988**, *110*, 1643−1644.

10.1021/cm070277z CCC: $37.00
Published on Web 06/30/2007

tetrahydroborate in 1,2-dimethoxyethane (dme).[15,16] The product may be purified by crystallization from diethyl ether or sublimation at 50 °C and 10^{-4} Torr.

2. Film Deposition. Film deposition is performed in an ultrahigh vacuum chamber with a base pressure of 5×10^{-9} Torr.[17] The precursor is a solid that sublimes at 25 °C in vacuum; to increase the vapor pressure, the precursor reservoir is maintained at 40 °C during growth. The precursor is delivered to the growth chamber through a 3.8 mm i.d. stainless steel tube with the assistance of a 10 sccm stream of argon as a carrier gas. The substrate used is highly conducting n-type Si(100) that is heated either radiatively (for low temperatures, 170−200 °C) or resistively by passing dc current through the Si (for higher temperatures, up to 900 °C). Native oxide is removed by dilute HF etching before loading the substrate in the vacuum chamber. The nucleation and growth of the thin films are monitored in situ using spectroscopic ellipsometry (SE) with a fixed incident angle of 70° and photon energy in the range 0.75−5.05 eV.

We have previously described in detail the analysis of MB_2 film nucleation, growth, surface roughness, and electrical conductivity based on SE data.[18] In brief, the SE data set is modeled using a multilayer model that includes the substrate, the film, and a surface roughness layer. The surface roughness layer is approximated as 50% material (TiB_2) and 50% void using the Bruggeman effective medium approximation (EMA).[19,20] The dielectric constants of the TiB_2 film are modeled using the Drude−Lorentz expression (Supporting Information).[21] The model allows us to extract, with high confidence, time-dependent values for the bulk film thickness and effective surface roughness.

For the measurement of sheet resistance or diffusion barrier properties, 350 nm of SiO_2 is thermally grown on the Si substrate prior to TiB_2 deposition.

3. Byproduct Characterization. Two methods were used to analyze the byproducts generated upon deposition from $Ti(BH_4)_3$(dme). Non-quantitative analyses were conducted by measuring the mass spectrum of the products exiting the hot zone; the spectra were acquired on a Dycor M200 quadrupole mass spectrometer with Faraday cup detector connected to the dynamically pumped deposition chamber by means of a 500 μm molecular leak valve (Ametek/Thermox Instruments). Semiquantitative analyses were conducted by placing samples of $Ti(BH_4)_3$(dme) under a static vacuum in a closed Pyrex tube. A temperature gradient ranging from 60 to 200 °C (or 250 °C) was established along the length of the tube, with the precursor initially located at the low-temperature end. Over the course of the experiment, the precursor sublimed within the tube and deposited a dark silvery film on the hotter surfaces. The gases were sampled by opening the tube at the end of the run. GCMS data were obtained on a Hewlett-Packard 5890 gas chromatograph with a 5970 series mass selective detector and a 30 m RSL-160 (5 μm thick polydimethylsiloxane film, 0.32 mm i.d., Alltech) capillary column. The injection conditions were as follows: head pressure = 3 psig, injection temperature = 280 °C, detector temperature = 300 °C, splitter rate = 65 mL/min. The column temperature program was 6 min at 25 °C, ramp 15 °C/min to 200 °C. All of the mass percentages are relative amounts based on integration of the gas chromatogram peaks. Retention times were confirmed by comparisons with authentic samples. The mass spectra were easily assigned on the basis of their characteristic fragmentation and isotope patterns.[22]

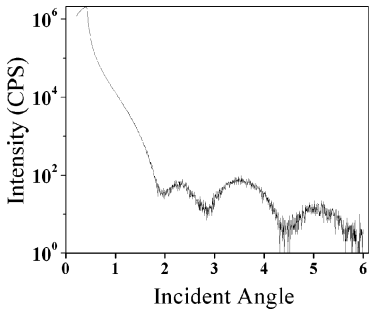

Figure 1. XRR measurement of a film grown at 175 °C for 1 min on SiO_2. Film thickness calculated from interference fringes is 5 nm.

Results and Discussion

1. Nucleation and Growth. The compound $Ti(BH_4)_3$(dme) is a volatile solid that, according to preliminary studies,[14] can serve as a single-source precursor to TiB_2 at temperatures near 250 °C. Using SE, we find that the threshold temperature for film deposition is 170 °C. At the onset of film growth, SE modeling shows an increase in the surface roughness to 2.6 nm without in increase in the bulk film thickness, which is a classic signature of the nucleation phase. (It is well documented that the effective roughness afforded by SE differs systematically from the root-mean-square (rms) roughness in atomic force microscopy (AFM) analyses.[23,24]) The delay between the start of precursor flow and the rise in initial film roughness (the nucleation delay)[18] is less than 30 s for films grown from $Ti(BH_4)_3$(dme) on SiO_2. Another indication of rapid nucleation is that a film grown for 1 min at 175 °C on SiO_2 has a thickness of 5 nm as measured by interference fringes from X-ray reflectivity (XRR) (Figure 1) and rms roughness of only 0.45 nm as measured by tapping mode AFM. Such a smooth and continuous film even after 1 min of growth is remarkable (i.e., far less than observed in comparable systems[18,25] and indicative of the ease of nucleation from this precursor). After nucleation is complete, the film thickness increases linearly with only a gradual increase in film roughness.

The atomic density of titanium atoms is calculated by dividing the area density, as obtained from Rutherford backscattering spectrometry (RBS), by the film thickness, measured from SEM images of fracture cross sections. We find that the titanium density decreases with increasing temperature (Figure 2, open circles), as is commonly observed for low-temperature CVD of other metal di-

(15) Franz, K.; Fusstetter, H.; Noth, H. *Z. Anorg. Allg. Chem.* **1976**, *427*, 97−113.
(16) Borisov, A. P.; Makhaev, V. D.; Lobkovskii, E. B.; Semenenko, K. N. *Zh. Neorg. Khim.* **1986**, *31*, 86−92.
(17) Jayaraman, S.; Klein, E. J.; Yang, Y.; Kim, D. Y.; Girolami, G. S.; Abelson, J. R. *J. Vac. Sci. Technol. A* **2005**, *23*, 631−633.
(18) Yang, Y.; Jayaraman, S.; Sperling, B.; Kim, D. Y.; Girolami, G. S.; Abelson, J. R. *J. Vac. Sci. Technol. A* **2007**, *25*, 200−206.
(19) Collins, R. W.; An, I.; Nguyen, H. V.; Gu, T. *Thin Solid Films* **1991**, *206*, 374−380.
(20) An, I.; Li, Y. M.; Nguyen, H. V.; Collins, R. W. *Rev. Sci. Instrum.* **1992**, *63*, 3842−3848.
(21) Hummel, R. E. *Electronic Properties of Materials*, 2nd ed.; Springer: Berlin, 1992.
(22) Shapiro, I.; Wilson, C. O.; Ditter, J. F.; Lehmann, W. J. *J. Adv. Chem. Ser.* **1961**, *32*, 127−138.
(23) Koh, J.; Lu, Y. W.; Wronski, C. R.; Kuang, Y. L.; Collins, R. W.; Tsong, T. T.; Strausser, Y. E. *Appl. Phys. Lett.* **1996**, *69*, 1297−1299.
(24) Sperling, B. A.; Abelson, J. R. *Appl. Phys. Lett.* **2004**, *85*, 3456−3458.
(25) Sung, J. W.; Goedde, D. M.; Girolami, G. S.; Abelson, J. R. *J. Appl. Phys.* **2002**, *91*, 3904−3911.

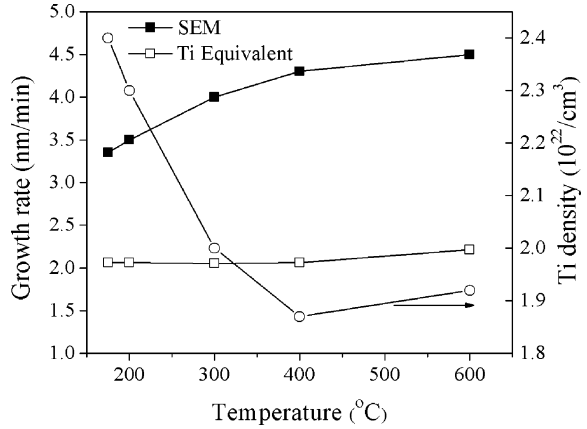

Figure 2. Film growth rate (solid squares), Ti-equivalent growth rate (open squares), and titanium atomic density (open circles) as a function of temperature.

Table 1. Volatile Byproducts from the CVD of TiB_2 from $Ti(BH_4)_3$(dme)[a]

T, *P*	dme	B_2H_6	C_2H_6	EtOMe	B_5H_9	Me_2O	C_3H_8
200 °C, 10^{-6} Torr	+	+	−	−	−	−	−
250 °C, 10^{-2} Torr	82.9	7.3	4.8	2.2	1.1	−	−
260 °C, 10^{-2} Torr	48.3	1.4	9.3	8.1	−	18.0	2.8

[a] Values shown are relative mole percentages; the measured values for diborane and pentaborane are expected to be low owing to reactions of these materials during passage through the GC/MS column.

borides.[17,26] Also shown in Figure 2 is the growth rate obtained from SEM data (solid squares) and the Ti-equivalent growth rate (open squares) obtained by dividing the measured Ti area density by the volume density of Ti in bulk TiB_2 and the growth time. The equivalent growth rate is constant for all temperatures. This result indicates that the reaction rate of the precursor molecules on the growth surface is faster than the rate of supply, that is, that growth is flux limited even at 170 °C under our conditions.[27] To check that the growth rate is flux limited, we increased the flux by heating the precursor reservoir to 50 °C; the growth rate increased by 50% at a substrate temperature of 250 °C. Flux-limited growth due to low precursor pressure is often reported for solid precursors.[28,29]

2. Analysis of Volatile CVD Products. The products formed when $Ti(BH_4)_3$(dme) is exposed to heated surfaces have been studied by MS and GC/MS methods (Table 1). At low temperatures (T < 250 °C) under flow conditions characteristic of a deposition process, the only product gases detected are dme and diborane, indicating that the dme ligands dissociate intact and undergo little fragmentation under these conditions. If the residence time of the products in the hot zone is increased, however, more products are observed. At 250 °C, 10^{-2} Torr pressure, and a 2 min residence time in the hot zone, dme and diborane are still the major products, but B_5H_9 and fragmentation products of the dme ligand (ethane, ethyl methyl ether) are also formed in small amounts (1−5 mol %): at a slightly higher deposition temperature of 260 °C with a 20 min residence time, the product distribution shows significant fragmentation of dme to generate larger amounts of the products above and also dimethyl ether and propene.

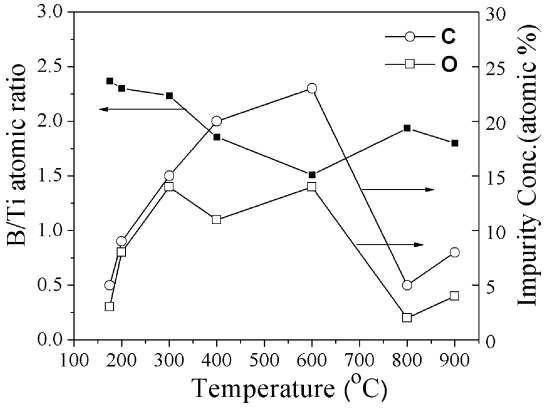

Figure 3. Boron to titanium atomic ratio (solid squares) and atomic concentration of carbon (open circles) and oxygen (open squares) as a function of growth temperature.

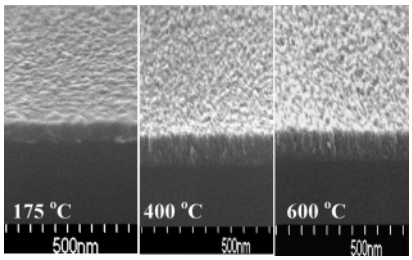

Figure 4. Cross-sectional SEM images of films grown at 175 °C, 400 °C, and 600 °C.

3. Composition. The B/Ti atomic ratio, as determined by Auger electron spectroscopy (AES) sputter profiling (Figure 3), is near stoichiometric at low growth temperatures (<200 °C). At intermediate temperatures (200−600 °C), the films are deficient in boron and contain significant amounts (>10 atomic % each) of carbon and oxygen. At 800 °C and above, the films are again stoichiometric and relatively free of impurities. The increase in the impurity concentration at intermediate temperatures is consistent with the results of the mass spectrometric study discussed in the previous section. Fragmentation of the dme ligand is responsible for the increased impurity concentrations and lowered boron levels in the films at these intermediate temperatures. A second mechanism, not understood at present, must be responsible for the low impurity content in films grown at the highest temperatures.

4. Microstructure. The microstructure, evaluated by cross-sectional SEM images (Figure 4), is dense columnar at growth temperatures of 175−200 °C and rough columnar at intermediate temperatures of 200−600 °C. The columnar morphology is a consequence of the low homologous temperatures, $T_{growth}/T_{melt} = 0.13-0.25$, at which the surface diffusion of adspecies is negligibly low. This microstructure is similar to that predicted by Thornton's zone diagram for sputter-deposited films.[30]

(26) Jayaraman, S.; Yang, Y.; Kim, D. Y.; Girolami, G. S.; Abelson, J. R. *J. Vac. Sci. Technol. A* **2005**, *23*, 1619−1625.
(27) Hampdensmith, M. J.; Kodas, T. T. *Chem. Vap. Deposition* **1995**, *1*, 8−23.
(28) Karpov, I.; Gladfelter, W.; Franciosi, A. *Appl. Phys. Lett.* **1996**, *69*, 4191−4193.
(29) Kodas, T. T.; Baum, T. H.; Comita, P. B. *J. Appl. Phys.* **1987**, *62*, 281−286.
(30) Thornton, J. A. *J. Vac. Sci. Technol. A* **1986**, *4*, 3059−3065.

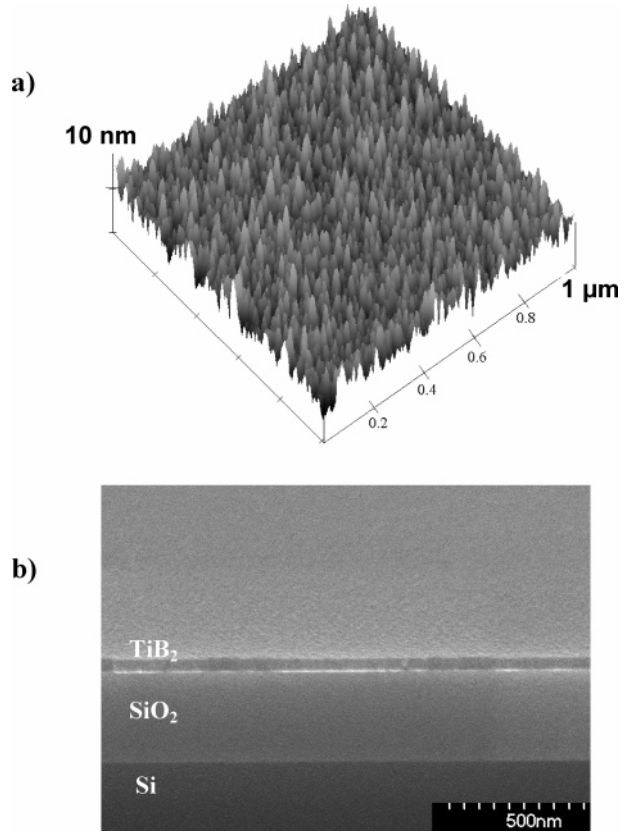

Figure 5. (a) AFM surface plot and (b) cross-sectional SEM images of a film grown on SiO_2 at 175 °C.

Low-temperature films grown on SiO_2 substrates are remarkably smooth, which we attribute to the ease of nucleation and the high density of nuclei on SiO_2. For a 50 nm thick film grown at 175 °C, the SEM cross-section is featureless and the AFM data correspond to a rms roughness of only 0.8 nm (Figure 5). At 175 °C the roughness remains below 1 nm for all film thicknesses measured, 5−60 nm. In contrast, a 50 nm thick film grown on silicon has a rms roughness of 1.6 nm, and films grown at higher temperatures (Figure 4) are rougher still.

5. Film Crystallinity. Films grown below 600 °C are amorphous as judged by X-ray diffraction. At 600 °C broad diffraction peaks (Figure 6) emerge from the background, which we interpret as evidence for nanocrystallites in an amorphous matrix. However, high-resolution TEM images of films deposited at 170 °C reveal lattice fringes from nanocrystallites 3−4 nm in diameter (Figure 7). The TEM diffraction pattern of the same sample (Figure 7, inset) shows continuous diffraction rings that index as TiB_2, but not as Ti or B, implying the presence of a large number of randomly oriented nanocrystallites. The very small size of the nanocrystallites explains the absence of X-ray diffraction peaks in films grown at lower temperature. The volume fraction of nanocrystallites and of any disordered phase (grain boundary or amorphous matrix) is difficult to quantify. Films deposited at 800 and 900 °C exhibit sharp diffraction features with preferred orientation. At 800 °C the film has a preferred (101) orientation on Si(001) (Figure 6); this is similar to the CVD growth of HfB_2 on Si(001) where the preferred

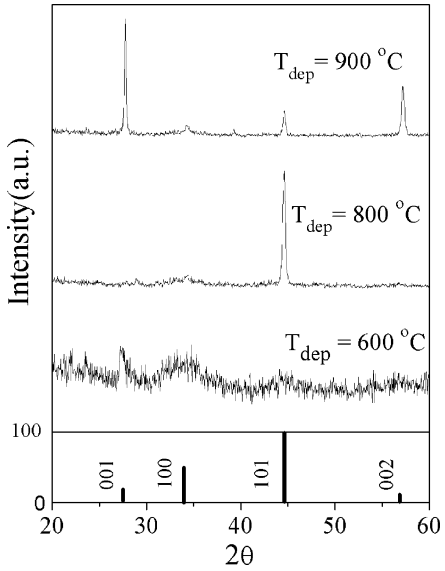

Figure 6. XRD profile of films grown at 600, 800, and 900 °C. The bottom of the figure shows a histogram of the ICCD X-ray powder diffraction pattern.

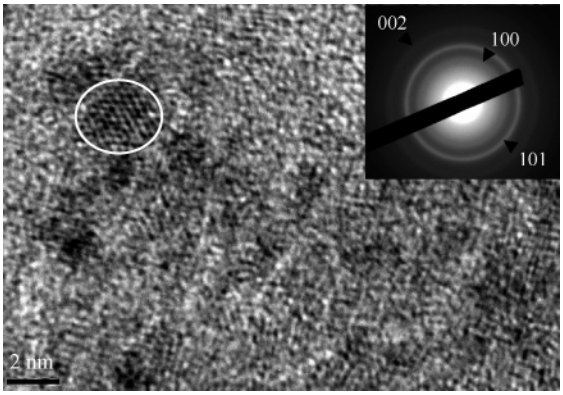

Figure 7. High-resolution TEM image of TiB_2 film grown on a Cu/SiO_2 grid at 175 °C; a nanocrystallite is shown encircled. Selected area electron diffraction pattern (SAED) of the same is shown in the inset with labeled TiB_2 lattice planes.

orientation is (101) at 800 °C.[31] At 900 °C the preferred orientation changes to (001). The change of orientation is also evident in the plan view SEM images which show a plate-like morphology for films grown at 800 °C (Figure 8a) and hexagonal facets (the basal plane of TiB_2) at 900 °C (Figure 8b). Auger sputter-profiling of these films shows the presence of silicon in the bulk for films grown at 800 and 900 °C but not at 600 °C or lower growth temperatures. The presence of silicon as detected by AES for 800 and 900 °C grown films can be attributed to the diffusivity of silicon and morphology of the films at these temperatures as has been observed and explained by Roucka et al.[32] in the growth of epitaxial ZrB_2 on silicon. At these temperatures, the incomplete coalescence of crystallites leaves voids in between the columnar crystallites. The surface silicon atoms which are highly mobile at these temperatures diffuses in these voids. Therefore, the presence of silicon in the bulk AES data for films grown at 800 and 900 °C is no surprise.

(31) Yang, Y.; Jayaraman, S.; Kim, D. Y.; Girolami, G. S.; Abelson, J. R. *J. Cryst. Growth* **2006**, *294*, 389−395.
(32) Roucka, R.; Tolle, J.; Chizmeshya, A. V. G.; Tsong, I. S. T.; Kouvetakis, J. *J. Cryst. Growth* **2005**, *277*, 364−371.

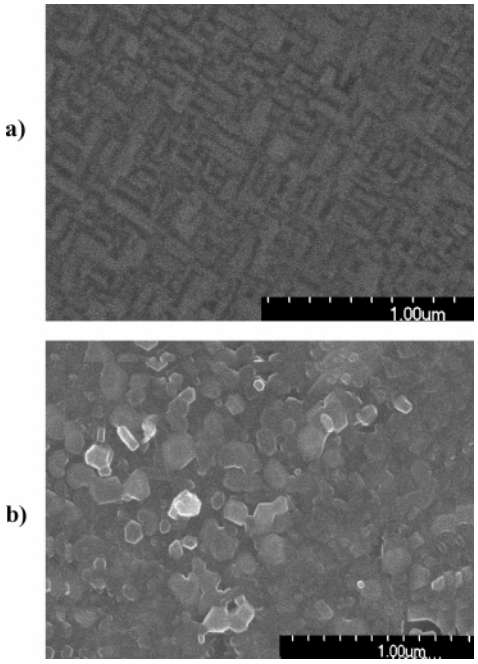

Figure 8. Plan view SEM images of films grown at (a) 800 °C and (b) 900 °C.

6. Diffusion Barrier Properties. Much research is being conducted to identify new and improved barrier materials to prevent copper diffusion in microelectronic devices. Such barriers must be extremely thin and should also form smooth interfaces with copper to provide minimum interfacial resistance in interconnect lines.[33] Stable nanocrystalline or amorphous diffusion barriers generally exhibit superior performance, apparently as a result of the lack of grain boundary diffusion pathways.[34]

The low-temperature TiB_2 films described in this paper are attractive for diffusion barrier applications owing to their amorphous structure and ability to form highly smooth films on SiO_2. Four-point probe measurements showed that a 40 nm thick TiB_2 film deposited at 175 °C had a resistivity of 275 $\mu\Omega$·cm. To test the barrier performance of this material, we evaporated 40 nm of copper on top of a 7 nm thick TiB_2 film grown at 175 °C on a SiO_2 substrate. This structure (40 nm Cu/7 nm TiB_2/350 nm SiO_2/Si) was annealed in vacuum for 30 min and then analyzed by RBS using 2 MeV He^+ ions to assess the stability of the interface and determine the onset of barrier failure. Figure 9 shows RBS profiles for as-deposited, 600 °C annealed and 700 °C annealed test structures; the positions of copper, titanium, silicon, and oxygen peaks in the as-deposited RBS profile are marked. The peak due to boron in TiB_2 is not resolved because the Rutherford scattering cross sections vary as the square of the atomic number, and the boron peak sits on top of the strong signal from the Si substrate. There is no observable change in the RBS profile for the test structures after it is annealed at 600 °C. However, for the film annealed at 700 °C, Figure 9 shows that the copper peak has attenuated and broadened to form a tail at lower scattering energies

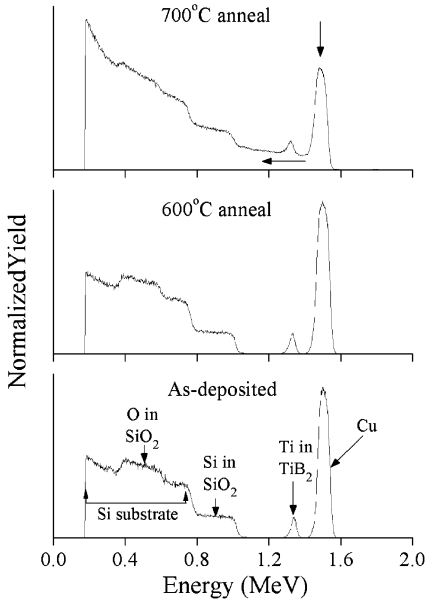

Figure 9. RBS profile from a diffusion test structure consisting of (40 nm) Cu/(7 nm) TiB_2/350 nm SiO_2/Si, as-deposited (bottom), vacuum-annealed at 600 °C for 30 min (middle), and vacuum-annealed at 700 °C for 30 min (top). The arrows in the 700 °C spectrum show the change in the shape of the copper peak due to diffusion deeper into the structure.

due to the diffusion of Cu through the TiB_2 barrier and deep into the SiO_2 and Si layers. To confirm this interpretation, RBS profile simulations were carried out using the fitting software RUMP.[35] Fitting of the 700 °C spectrum suggests that the Cu concentration is ~0.15 atom % in the SiO_2 layer and ~0.1 atom % in the near-surface Si layer. The RBS data indicates that TiB_2 diffusion barrier fails after a 700 °C anneal. A similar failure at 700 °C was reported for a 60 nm thick sputtered TiB_2 diffusion barrier.[6] In fact, a wide variety of diffusion barrier materials, including thicker layers, have been reported to fail at this temperature.[36,37]

Conclusions

We present a low temperature and halogen free CVD route to deposit high quality TiB_2. Films deposition starts at 170 °C, and the low-temperature films (<600 °C) are X-ray amorphous. The films nucleate remarkably well on oxide substrate. Low-temperature films grown on SiO_2 are highly smooth and have rms roughness below 1 nm for thickness from 5 to 60 nm. High-temperature films (800 and 900 °C) are crystalline and have preferred orientation with the substrate. The film stoichiometry at low and intermediate temperatures is in agreement with the mass spectroscopy results presented for the precursor. A 7 nm film tested as a diffusion barrier was able to resist Cu diffusion at 600 °C for 30 min.

Acknowledgment. The authors are grateful to the National Science Foundation for support of this research under Grants

(33) International Technology Roadmap for Semiconductors. http://public.itrs.net (accessed 2005).
(34) Kaloyeros, A. E.; Eisenbraun, E. *Annu. Rev. Mater. Sci.* **2000**, *30*, 363−385.
(35) Doolittle, L. R. *Nucl. Instr. Methods Phys. Res., Sect. B* **1985**, *9*, 344−351.
(36) Kim, H.; Cabral, C.; Lavoie, C.; Rossnagel, S. M. *J. Vac. Sci. Technol. B* **2002**, *20*, 1321−1326.
(37) Cho, S. L.; Kim, K. B.; Min, S. H.; Shin, H. K.; Kim, S. D. *J. Electrochem. Soc.* **1999**, *146*, 3724−3730.

NSF CH 00-76061, NSF DMR 03-15428, and NSF 04-20768. The authors would also like to thank James A. Jensen and John E. Gozum for their contribution towards the data in Table 1. Compositional and structural analyses of the films were carried out in the Center for Microanalysis of Materials, University of Illinois, which is partially supported by the U.S. Department of Energy under Grant DEFG02-91-ER45439.

Supporting Information Available: Description of dielectric constants of TiB_2 modeled by the Drude−Lorentz expression and table of parameters that provide a best fit to the ellipsometry data (PDF). This material is available free of charge via the Internet at http://pubs.acs.org.

CM070277Z